

Elastic constants and mechanical properties of PEDOT from first principles calculations

R. O. Agbaoye^a, P. O. Adebambo^b, J. O. Akinlami^a, T. A. Afolabi^c, Smagul Zh. Karazhanov^d, Davide Ceresoli^{e,*}, G. A. Adebayo^{a,*}

^a*Department of Physics, Federal University of Agriculture, PMB 2240, Abeokuta, Nigeria*

^b*Department of Physical and Computer Sciences, McPherson University, Abeokuta, Nigeria*

^c*Department of Chemistry, Federal University of Agriculture, PMB 2240, Abeokuta, Nigeria*

^d*Department for Solar Energy, Institute for Energy Technology, P.O Box 40, NO 2027-Kjeller, Norway*

^e*CNR-ISTM and INSTM, c/o Dipartimento di Chimica, Università degli studi di Milano, via Golgi 19, 20133 Milano, Italy*

Abstract

In this work, we report about the electronic and elastic properties of crystalline poly(3,4-ethylenedioxythiophene), known as PEDOT, in an undiluted state, studied in the framework of semilocal DFT, using the PBE and PBEsol exchange-correlation functional and PAW pseudopotentials. Contrary to previous molecular dynamics simulations, our calculations revealed that the most stable state structure of pristine PEDOT is monoclinic. We calculated the 13 independent elastic constants and the elastic compliance which enables us to establish other elastic properties of pristine PEDOT; the Pugh's ratio and the Vicker's hardness computed with PBE and PBEsol are in good agreement with each other. Finally, we compute the directional elastic moduli and found remarkable differences between different DFT functionals.

Keywords: Density Functional Theory, Elastic properties, Polymer electronics, PEDOT

1. Introduction

As an organic semiconducting polymer, poly(3,4-ethylenedioxythiophene) (PEDOT) is finding highly significant applications in modern day technology. PEDOT, when doped with other polymers/materials, provides the ground to develop novel functional materials. Due to its flexible nature, thin films of PEDOT:PSS (PSS = polystyrene sulfonate) are being employed in flexible electronic devices [1]. Since the first synthesis of PEDOT [2], several experimental studies have been carried out on doped and pristine either as thin-film or bulk material. These studies range from synthesis, doping, chemical preparation, thermoelectric properties to the electronic, optical and structural determination. [1–7] The conductivity, atmospheric stability, band gap, thermoelectric figure of merit among other properties of PEDOT have improved over time, but the elastic and thermodynamics properties have neither been studied nor reported until now. [8, 9].

*Corresponding author

Email addresses: agbaoye@physics.unaab.edu.ng (R. O. Agbaoye), adebambo@physics.unaab.edu.ng (P. O. Adebambo), johnsonak2000@yahoo.co.uk (J. O. Akinlami), afolabita@funaab.edu.ng (T. A. Afolabi), smagul.karazhanov@ife.no (Smagul Zh. Karazhanov), davide.ceresoli@cnr.it (Davide Ceresoli), adebayo@physics.unaab.edu.ng (G. A. Adebayo)

As mentioned earlier, PEDOT is an optically active conductive conjugated polymer [3]. It exists as an organic semiconductor with a small direct band gap in the pure state; with exceptional environmental stability and electrical conductivity [4–7]. Synthesis in the pristine state via chemical polymerization results in blue-black color, while it becomes to almost transparent when doped [5, 6]. This is due to the ability to change from benzoic shape to quinoid structure when doped with PSS and from aromatic-like structure to quinoid-like structure when doped with tosylate [8–11]. In pristine, undoped PEDOT, the gap between its highest occupied molecular orbital (HOMO) and its lowest unoccupied molecular orbitals (LUMO) is reported as 1.5 eV [6], 1.6–1.7 eV [7] and 1.64 eV [12]. On the other hand, Refs. [8, 9, 11] report band gaps of 0.37 eV with the B3LYP exchange-correlation functional, 0.45 eV with PBE, 0.16 eV with PBE-D and 0.53 eV with the HSE06 hybrid functional. The discrepancy between the experimental and theoretical band gap might be related to the fact that experimental measurements are carried on dispersed PEDOT in thin films, while the theoretical calculations address only the pure crystalline phases.

These important attributes of PEDOT make it an important material to be studied both theoretically and experimentally. Recent calculations by Wen Shi et al. [8] provided electronic and thermoelectric properties of both pristine and doped PEDOT. A theoretical investigation of the mechanical properties and how they influence the electrical conductivity of PEDOT, will shed more light on the efficiency and reliability of PEDOT for flexible-electronic applications. As a first step towards elucidating this, we calculated the elastic constants and mechanical properties of PEDOT, and thermodynamic properties (Debye temperature, specific heat capacity) by first principles DFT lattice dynamics calculations.

To compute elastic properties, in principle one has to deal with 81 independent elastic constants associated with a crystal. However, using the approach employed by Newman, these are reduced to 21 for all crystal structure [13]; the symmetry operations of a monoclinic crystal contribute to reducing the 21 independent elastic constants down to 13. Using the Voigt notation, the elastic constants tensor for a monoclinic b unique axis crystal can be written as:

$$C = \begin{bmatrix} C_{11} & C_{12} & C_{13} & 0 & C_{15} & 0 \\ & C_{22} & C_{23} & 0 & C_{25} & 0 \\ & & C_{33} & 0 & C_{35} & 0 \\ \vdots & & & C_{44} & 0 & C_{46} \\ & \ddots & & & C_{55} & 0 \\ & & \dots & & & C_{66} \end{bmatrix}, \quad (1)$$

where the dots mean that the matrix is symmetric.

From the elastic constants, one can determine various elastic moduli: the shear modulus, Young modulus, the Poisson ratio, and the bulk modulus [13–15]. The Poisson ratio gives information about the type of bond that is possess in any material which later predicts the properties of such material when a load is exerted

on it [14]. A Poisson ratio within the range 0.25–0.42 characterizes a material dominated by metallic bonding [15]. In glasses, ceramics and semiconductors, the Poisson ratio is close to 0.25. However, Greaves and co-workers predicted a Poisson ratio approximately 0.33 in polymers [14]. Therefore, understanding how PEDOT is classified, in terms of mechanical properties, is extremely interesting.

2. Computational methods

Experimentally, PEDOT is semicrystalline and can be obtained with different degrees of crystallinity. Despite the fact that X-ray diffraction experiments [6, 7] display sharp peaks, corresponding to the lamellar structure of the polymer, the crystalline structure of undoped PEDOT has not been fully determined (only lattice parameters assuming an orthorhombic structure have been reported).

[Figure 1 about here.]

Previous DFT calculations, have shown that the crystal structure of PEDOT can be either orthorhombic [9–11], or monoclinic [8]. In the present work, we started from the monoclinic structure of Ref. [8] (space group $P2/c$) of pristine-type PEDOT, and performed full relaxation of the lattice.

We used two semilocal exchange and correlation functionals, the PBE [16] and PBEsol [17]. In PBE calculations we used norm-conserving pseudopotentials¹ and a plane wave cutoff of 120 Ry. In PBEsol calculations we used PAW pseudopotentials², from *PSlibrary* [18] and 75 Ry (750 Ry) energy cutoff for the planewaves (density). Together with a Monkhorst-Pack k-points grid of $4\times 7\times 8$ points, this setup leads to well converged total energy within 0.8 meV/atom. The k-points grid was chosen in order to sample the reciprocal space most uniformly possible, along the three reciprocal lattice vectors.

The optimization calculations were performed for both monoclinic and orthorhombic crystal structures, these calculations revealed the most stable phase of monoclinic pristine PEDOT. We initially performed the variable-cell relaxation with a smaller k-point mesh ($2\times 4\times 4$) and then, to reduce the force on the ions and to obtain the most stable state at minimum energy, the angle β between the lattice parameters a and c was optimized to achieve a global minimum state of the crystal using the finer $4\times 7\times 8$ kpoint grid. Finally, we performed a self-consistent field (SCF) single point calculation with a $6\times 10\times 11$ k-point mesh and calculated the electronic band structure along the high symmetry lines of the Brillouin Zone. To obtain a smooth density of states (DOS), we performed non-SCF with a denser Monkhorst-Pack grid of $7\times 11\times 12$.

We calculated the elastic constants of the molecular PEDOT by exerting strains that cause either longitudinal, transverse or both longitudinal and transverse distortion to the system, thereby calculating the stress that takes it back to its initial configuration, the strain and the obtained stress are then fitted to get

¹C.pbe-nc.UPF, O.pbe-nc.UPF, S.pbe-n-nc.UPF, H.pbe-n-nc.UPF

²C.pbesol-n-kjpaw_psl.0.1.UPF, O.pbesol-n-kjpaw_psl.0.1.UPF, S.pbesol-n-kjpaw_psl.0.1.UPF, H.pbesol-kjpaw_psl.0.1.UPF

the 13 independent elastic constants. Since the energy derivatives are more sensitive to the convergence parameters, we calculated the elastic constants with a $2 \times 4 \times 4$, $3 \times 5 \times 5$, $4 \times 7 \times 8$, $5 \times 8 \times 9$, $6 \times 9 \times 10$ and $7 \times 11 \times 12$ Monkhorst-Pack grid. These correspond to 18, 24, 72, 115, 204, 258 k-points and 20, 38, 114, 181, 332, 463 k-points for PBE and PBEsol.

The elastic constants are calculated using the finite difference approach [19]. The small strain ϵ_j applied to perturb a crystal, and the stress tensor α_j that tends to return it to equilibrium, are related by:

$$\alpha_j = \sum_{i=1}^6 C_{ij} \epsilon_i \quad (2)$$

We perturbed the crystal by a set of 3×3 strain tensors which varies the length of lattice parameters, the size of the crystal along the yz , xz , xy planes, for a small applied strain (ϵ) of magnitude -0.0075 , -0.0025 , 0.0025 and 0.0075 . Then, elastic constants are calculated [16-18, 20] from Voigt-Heuss-Hill approximation. Then, we calculated bulk modulus, Young modulus, shear modulus and the Poisson ratio for PEDOT using the approach described in Refs. [15, 20, 21]. Other calculated properties are the Pugh's modulus ratio and Vicker's hardness [1, 22-24]. This method, although computationally expensive, has proven to be very accurate method of determining the elastic properties of both organic and inorganic crystals [25] with respect to other methods [22]. Finally, we calculated the dependence of the elastic moduli on the spatial direction, according to Ref. [26].

3. Results and discussion

The lattice parameters a , b , c and monoclinic angle β are reported in Tab. 1, together with experimental data and previous calculations. The orthorhombic structures can be seen as monoclinic by the following transformation:

$$\vec{a}' = \vec{a} + \vec{c}, \quad \vec{b}' = \vec{b}, \quad \vec{c}' = \vec{c}, \quad (3)$$

where a' , b' and c' are lattice spacings of the orthorhombic structure. In Tab. 1, for sake of comparison, for the orthorhombic structures, we report also the corresponding monoclinic lattice parameters, as well as the crystal cell volume. The b -unique monoclinic crystal structure of pristine PEDOT [8] consists of four units of ethylene dioxythiophene (EDOT), arranged into two parallel polymeric chains as illustrated in Fig. 1.

[Table 1 about here.]

Despite being in the reported experimental range, the optimized lattice parameters using the PBE and PBEsol exchange-correlation functionals overestimates the volume of the system. This is to be expected, since the PBE family is known to under-bind a large class of systems, molecular and periodic. Even if PBEsol was designed specifically to reproduce the lattice spacing of inorganic systems, it is still unable to describe

the weak dispersion forces that characterize molecular and polymeric crystals. For instance, polyethylene crystal was predicted to be unbound using the semilocal BLYP functional and it could be stabilized by the inclusion of an empirical term. [27] From Tab. 1 it is evident that van der Waals and dispersion forces are essential to describe the cohesive energy of crystalline PEDOT. Therefore we employed the empirical correction (+D2) proposed by Grimme [28]. The b lattice parameter (parallel to the polymer chains, where chemical bonding is covalent) is well described both by PBE and PBEsol, with and without vdW corrections. Notably, the difference between the PBE+D2 and PBEsol+D2 equilibrium volume is $\sim 6\%$.

[Figure 2 about here.]

After obtaining the optimized lattice parameters a , b , c and β , we calculate the equation of state of PEDOT by computing the energy versus volume curve. At its minimum energy, the equilibrium volume is 534.36 \AA^3 for PBE and 501.22 \AA^3 for PBEsol, both including the Grimme+D2 correction [28]. The results are shown in Fig. 2. The good convergence (cutoff and k-points sampling) of our calculations is supported by the fact that the calculated pressure (from the trace of stress tensor) vanishes at equilibrium.

[Figure 3 about here.]

We calculated direct band gaps of 0.32 eV and 0.42 eV respectively in PBEsol and PBE exchange-correlation functionals. In both cases, flat-bands occur between 2 to 3 eV and between -4 to -5 eV, which are due to the absence of electron hopping at those energies, and manifest as sharp peaks in the density of state plot. The density of states at the valence and conduction band edges is quite small, and the band structure displays an oval-shaped band from Γ to Z , with nearly symmetric valence and conduction dispersion. The bands also show significant band gaps at the Y and Q high symmetry points. The band structures are similar to what was reported in Refs. [8, 9, 11]. In this work, PBE exchange-correlation functional produces a larger band gap. This variation in band gap is due to the difference in the exchange-correlation term supplied to the Kohn-Sham equation within DFT. Although there is no report on the experimental band gap of bulk pristine PEDOT, from the study of Ref. [29], PBEsol predicted a small band gap from DFT study of some oxyfluoride compounds. The calculated PBE and PBEsol-PAW band gaps in this work are in good agreements with 0.45 eV reported in Ref. [9] and 0.37 eV computed by Kim [11], although far from 0.53 eV and 0.16 eV reported in Ref. [8].

DFT is in principle exact, the issue is with the exchange-correlation (XC) functionals. It is a well known fact that local and semilocal XCs (such as LDA and GGAs) severely underestimates band gaps by a factor ~ 2 in most systems, but from Tab. 2 it is apparent that the underestimation is much more dramatic in the present case. Hybrid-DFT functionals (such as HSE06) are known to mitigate this problem and yield gaps larger than the PBE family. In fact, the largest band gap in Tab. 2 has been obtained with HSE06. However, from Tab. 1, the crystal structure obtained by Shi and co-workers, overestimates the lattice spacing (hence

the volume) of the crystal, and this results in a band gap reduction. For a reliable estimate of crystalline PEDOT band gap, one could perform a GW-BSE [30] calculation, on the equilibrium volume that is found by PBE and PBEsol. Indeed, Ref. [31], report that the GW-BSE band gap of several conjugated polymers is roughly 2.2-2.5 larger than that of PBE.

[Table 2 about here.]

[Figure 4 about here.]

[Table 3 about here.]

We calculated the converged 13 independent elastic constants, with respect to k-point sampling (Fig. 4 and Tab. 3). The difference between PBEsol and PBE are mainly related to the small differences in the lattice spacing. Moreover, it is a well-known fact that PBE tends to underestimate crystal cohesive energy and elastic moduli. In the present case, PBE yields negative off-diagonal elastic constants. A negative elastic constant is not forbidden, as long as it fulfills all the Cauchy relations for mechanical stability [32]. Indeed, both PBE and PBEsol elastic constant matrices have positive eigenvalues, which is the necessary and sufficient condition for the mechanical stability. Our results show a similar trend to the ones reported in Ref. [33], calculated for the β -cyclotetramethylene tetranitramine molecular crystal.

[Figure 5 about here.]

[Table 4 about here.]

From the elastic constants, we extracted the averaged Hill elastic moduli and as well as the Poisson ratio [34]. Our results, highlight the importance of k-point sampling in computing elastic properties. In fact, while a relatively coarse k-point sampling is sufficient to converge the total energy, converging derivatives of the total energy (forces and stress) usually require finer k-point meshes. With PBEsol, we reach convergence after 463 k-points resulting in a maximum 0.08% difference in the moduli with respect to 332 k-points. Similarly, with PBE and using norm-conserving pseudopotentials, 258 k-points yield 1-3% variation in the moduli, compared to 204 k-points. Due to the large number of k-point, these calculations required a substantial computational effort. The Pugh ratio shows a disagreement on its brittleness as PBEsol categorize pristine PEDOT as ductile while PBE calculations predict a brittle material with a greater Vickers hardness. With a hardness of 1.77 kbar and 1.94 kbar, PEDOT is far from that of diamond which is a super-hard material but has its hardness similar to that of ZnS with experimental Vicker's Hardness of 18 kbar [23, 35]. Since the ratio of Bulk Modulus to Shear Modulus is greater than unity, and the Poisson ratio tends weakly towards 0.5, we predict pristine PEDOT as mildly incompressible.

In Fig. 4, one can note that the C_{33} and C_{35} elastic constants are not fully converged with respect to k-points sampling. In principle it is possible to calculate the error propagation from the elastic constants, to

the Hill elastic moduli. However, to have an estimate, we computed the change of elastic moduli due to a variation of the C_{33} (from 336 to 420 kbar) and C_{35} (from 87 to 100 kbar) elastic constants. We found that these variations have a small effect on the Hill moduli. The maximum variation of the bulk, Young and shear modulus is 6, 10 and 4 kbar, respectively. The Poisson ratio remains basically unchanged. Therefore, the large difference between the PBE+D2 and PBEsol+D2 calculated elastic moduli can be explained by the large difference between the elastic constants, and not by the uncertainty of the individual elastic constants

For highly anisotropic materials, it is instructive to report the directional elastic moduli (see Fig. 6). The Young modulus is largest in the y direction, parallel to the polymer chain, both for PBE+D2 and PBEsol+D2. However, the linear compressibility behaves differently. It is largest for PBEsol+D2 in the xz plane, with an angle of -45° with the x axis. This means that in PBEsol+D2 it's easier to compress the polymer *lamella* along in the π - π stacking direction, and to reduce the inter-chain distance (see also Fig. 1). Conversely, the PBE+D2 functional predict that PEDOT is more compressible along the x direction, such to reduce the distance between chains which are co-planar. Finally, the Shear modulus behaves similarly with the two XC functionals. Mechanical experiments on highly crystalline, fiber oriented PEDOT, might help to ascertain which functional is better in describing the elastic properties of PEDOT.

[Figure 6 about here.]

4. Conclusions

This paper presents a study of ground state properties, elastic and thermodynamic properties of crystalline PEDOT. Our results are in relatively good agreement with experimental data. The mismatch in the Pugh ratio that results in classifying pristine PEDOT as ductile and brittle with different functionals and pseudopotentials is open to debate. We predicted pristine PEDOT is mildly incompressible. Our results provide new physical insights to the elastic and mechanical properties of PEDOT.

Acknowledgments

The authors acknowledge the Abdus Salam International Centre for Theoretical Physics for computational access to its Clusters, ROA and GA are grateful to Ivan Girotto for assistance on resolving computational bugs. DC acknowledges Alberto Bossi (CNR-ISTM) and Donato Belmonte (University of Genova) for useful discussions.

- [1] J. Zhou, D. H. Anjum, L. Chen, X. Xu, I. A. Ventura, L. Jiang, G. Lubineau, The temperature-dependent microstructure of pedot/pss films: insights from morphological, mechanical and electrical analyses, *J. Mater. Chem. C* 2 (2014) 9903–9910. doi:10.1039/C4TC01593B. URL <http://dx.doi.org/10.1039/C4TC01593B>

- [2] B. Cho, K. S. Park, J. Baek, H. S. Oh, Y.-E. Koo Lee, M. M. Sung, Single-crystal poly(3,4-ethylenedioxythiophene) nanowires with ultrahigh conductivity, *Nano Letters* 14 (6) (2014) 3321–3327. doi:10.1021/nl500748y.
URL <http://dx.doi.org/10.1021/nl500748y>
- [3] W. Cho, J. Wu, B. S. Shim, W.-F. Kuan, S. E. Mastroianni, W.-S. Young, C.-C. Kuo, T. H. Epps, III, D. C. Martin, Synthesis and characterization of bicontinuous cubic poly(3,4-ethylene dioxythiophene) gyroid (pedot gyr) gels, *Phys. Chem. Chem. Phys.* 17 (2015) 5115–5123. doi:10.1039/C4CP04426F.
URL <http://dx.doi.org/10.1039/C4CP04426F>
- [4] O. Pyshkina, A. Kubarkov, V. Sergeyev, Poly(3,4-ethylenedioxythiophene): synthesis and properties, in: *Scientific Journal of Riga Technical University, Material Science and Applied Chemistry*, Vol. 21, Riga Technical University Latvia, Riga, 2010, pp. 51–54.
- [5] Q. Pei, G. Zuccarello, M. Ahlskog, O. Ingans, Electrochromic and highly stable poly(3,4-ethylenedioxythiophene) switches between opaque blue-black and transparent sky blue, *Polymer* 35 (7) (1994) 1347 – 1351. doi:[http://dx.doi.org/10.1016/0032-3861\(94\)90332-8](http://dx.doi.org/10.1016/0032-3861(94)90332-8).
URL <http://www.sciencedirect.com/science/article/pii/0032386194903328>
- [6] F. Tran-Van, S. Garreau, G. Louarn, G. Froyer, C. Chevrot, Fully undoped and soluble oligo(3,4-ethylenedioxythiophene)s: spectroscopic study and electrochemical characterization, *J. Mater. Chem.* 11 (2001) 1378–1382. doi:10.1039/B100033K.
URL <http://dx.doi.org/10.1039/B100033K>
- [7] K. Aasmundtveit, E. Samuelsen, L. Pettersson, O. Ingans, T. Johansson, R. Feidenhans'l, Structure of thin films of poly(3,4-ethylenedioxythiophene), *Synthetic Metals* 101 (1) (1999) 561 – 564. doi:[http://dx.doi.org/10.1016/S0379-6779\(98\)00315-4](http://dx.doi.org/10.1016/S0379-6779(98)00315-4).
URL <http://www.sciencedirect.com/science/article/pii/S0379677998003154>
- [8] W. Shi, T. Zhao, J. Xi, D. Wang, Z. Shuai, Unravelling doping effects on pedot at the molecular level: From geometry to thermoelectric transport properties, *Journal of the American Chemical Society* 137 (40) (2015) 12929–12938. doi:10.1021/jacs.5b06584.
URL <http://dx.doi.org/10.1021/jacs.5b06584>
- [9] B. Zhang, K. Wang, D. Li, X. Cui, Doping effects on the thermoelectric properties of pristine poly(3,4-ethylenedioxythiophene), *RSC Adv.* 5 (2015) 33885–33891. doi:10.1039/C4RA16451B.
URL <http://dx.doi.org/10.1039/C4RA16451B>
- [10] A. Lenz, H. Kariis, A. Pohl, P. Persson, L. Ojamäe, The electronic structure and reflectivity of pedot:pss from density functional theory, *Chemical Physics* 384 (13) (2011) 44 – 51. doi:<http://doi.org/10.1016/j.chemphys.2011.05.003>.
URL <http://www.sciencedirect.com/science/article/pii/S0301010411001571>
- [11] E.-G. Kim, J.-L. Brdas, Electronic evolution of poly(3,4-ethylenedioxythiophene) (pedot): From the isolated chain to the pristine and heavily doped crystals, *Journal of the American Chemical Society* 130 (50) (2008) 16880–16889. doi:10.1021/ja806389b.
URL <http://dx.doi.org/10.1021/ja806389b>
- [12] E. E. Havinga, C. M. J. Mutsaers, L. W. Jenneskens, Absorption properties of alkoxy-substituted thienylenevinylene oligomers as a function of the doping level, *Chemistry of Materials* 8 (3) (1996) 769–776. doi:10.1021/cm9504551.
URL <http://dx.doi.org/10.1021/cm9504551>
- [13] N. R. E., *Properties of Materials: Anisotropy, Symmetry, Structure*, Oxford University Press, 2005.
- [14] G. N. Greaves, A. L. Greer, R. S. Lakes, T. Rouxel, Poisson's ratio and modern materials, *Nature Materials* 10 (11) (2011) 823–837. doi:10.1038/nmat3134.
URL <http://dx.doi.org/10.1038/nmat3134>
- [15] Y. Li, Y. Gao, B. Xiao, T. Min, Y. Yang, S. Ma, D. Yi, The electronic, mechanical properties and theoretical hardness

- of chromium carbides by first-principles calculations, *Journal of Alloys and Compounds* 509 (17) (2011) 5242 – 5249. doi:<http://doi.org/10.1016/j.jallcom.2011.02.009>.
URL <http://www.sciencedirect.com/science/article/pii/S0925838811003197>
- [16] J. P. Perdew, K. Burke, M. Ernzerhof, Generalized gradient approximation made simple, *Phys. Rev. Lett.* 77 (1996) 3865–3868. doi:10.1103/PhysRevLett.77.3865.
URL <https://link.aps.org/doi/10.1103/PhysRevLett.77.3865>
- [17] J. P. Perdew, A. Ruzsinszky, G. I. Csonka, O. A. Vydrov, G. E. Scuseria, L. A. Constantin, X. Zhou, K. Burke, Restoring the density-gradient expansion for exchange in solids and surfaces, *Phys. Rev. Lett.* 100 (2008) 136406. doi:10.1103/PhysRevLett.100.136406.
URL <https://link.aps.org/doi/10.1103/PhysRevLett.100.136406>
- [18] A. D. Corso, Pseudopotentials periodic table: From h to pu, *Computational Materials Science* 95 (2014) 337 – 350. doi:<http://doi.org/10.1016/j.commatsci.2014.07.043>.
URL <http://www.sciencedirect.com/science/article/pii/S0927025614005187>
- [19] R. Golesorkhtabar, P. Pavone, J. Spitaler, P. Puschnig, C. Draxl, Elastic: A tool for calculating second-order elastic constants from first principles, *Computer Physics Communications* 184 (8) (2013) 1861 – 1873. doi:<http://doi.org/10.1016/j.cpc.2013.03.010>.
URL <http://www.sciencedirect.com/science/article/pii/S0010465513001070>
- [20] A. D. Corso, Elastic constants of beryllium: a first-principles investigation, *Journal of Physics: Condensed Matter* 28 (7) (2016) 075401.
URL <http://stacks.iop.org/0953-8984/28/i=7/a=075401>
- [21] R. Shahsavari, M. J. Buehler, R. J.-M. Pellenq, F.-J. Ulm, First-principles study of elastic constants and interlayer interactions of complex hydrated oxides: Case study of tobermorite and jennite, *Journal of the American Ceramic Society* 92 (10) (2009) 2323–2330. doi:10.1111/j.1551-2916.2009.03199.x.
URL <http://dx.doi.org/10.1111/j.1551-2916.2009.03199.x>
- [22] E. Güler, M. Güler, Elastic and mechanical properties of hexagonal diamond under pressure, *Applied Physics A* 119 (2) (2015) 721–726. doi:10.1007/s00339-015-9020-8.
URL <http://dx.doi.org/10.1007/s00339-015-9020-8>
- [23] Y. Tian, B. Xu, Z. Zhao, Microscopic theory of hardness and design of novel superhard crystals, *International Journal of Refractory Metals and Hard Materials* 33 (2012) 93 – 106. doi:<http://doi.org/10.1016/j.ijrmhm.2012.02.021>.
URL <http://www.sciencedirect.com/science/article/pii/S026343681200042X>
- [24] C. Lechner, B. Pannier, P. Baranek, N. C. Forero-Martinez, H. Vach, First-principles study of the structural, electronic, dynamic, and mechanical properties of hopg and diamond: Influence of exchange–correlation functionals and dispersion interactions, *The Journal of Physical Chemistry C* 120 (9) (2016) 5083–5100. doi:10.1021/acs.jpcc.5b10396.
URL <http://dx.doi.org/10.1021/acs.jpcc.5b10396>
- [25] H. Yao, L. Ouyang, W.-Y. Ching, Ab initio calculation of elastic constants of ceramic crystals, *Journal of the American Ceramic Society* 90 (10) (2007) 3194–3204. doi:10.1111/j.1551-2916.2007.01931.x.
URL <http://dx.doi.org/10.1111/j.1551-2916.2007.01931.x>
- [26] R. Gaillac, P. Pullumbi, F.-X. Coudert, Elate: an open-source online application for analysis and visualization of elastic tensors, *Journal of Physics: Condensed Matter* 28 (27) (2016) 275201.
URL <http://stacks.iop.org/0953-8984/28/i=27/a=275201>
- [27] S. Serra, S. Iarlori, E. Tosatti, S. Scandolo, G. Santoro, Dynamical and thermal properties of polyethylene by ab initio simulation, *Chemical Physics Letters* 331 (24) (2000) 339 – 345. doi:[https://doi.org/10.1016/S0009-2614\(00\)00881-2](https://doi.org/10.1016/S0009-2614(00)00881-2).
URL <http://www.sciencedirect.com/science/article/pii/S0009261400008812>

- [28] S. Grimme, Density functional theory with london dispersion corrections, Wiley Interdisciplinary Reviews: Computational Molecular Science 1 (2) (2011) 211–228. doi:10.1002/wcms.30.
URL <http://dx.doi.org/10.1002/wcms.30>
- [29] N. Charles, J. M. Rondinelli, Assessing exchange-correlation functional performance for structure and property predictions of oxyfluoride compounds from first principles, Phys. Rev. B 94 (2016) 174108. doi:10.1103/PhysRevB.94.174108.
URL <https://link.aps.org/doi/10.1103/PhysRevB.94.174108>
- [30] M. L. Tiago, J. R. Chelikowsky, First-principles gwbse excitations in organic molecules, Solid State Communications 136 (6) (2005) 333 – 337. doi:<http://doi.org/10.1016/j.ssc.2005.08.012>.
URL <http://www.sciencedirect.com/science/article/pii/S003810980500712X>
- [31] A. Ferretti, G. Mallia, L. Martin-Samos, G. Bussi, A. Ruini, B. Montanari, N. M. Harrison, Ab initio, Phys. Rev. B 85 (2012) 235105. doi:10.1103/PhysRevB.85.235105.
URL <https://link.aps.org/doi/10.1103/PhysRevB.85.235105>
- [32] F. Mouhat, F. m. c.-X. Coudert, Necessary and sufficient elastic stability conditions in various crystal systems, Phys. Rev. B 90 (2014) 224104. doi:10.1103/PhysRevB.90.224104.
URL <https://link.aps.org/doi/10.1103/PhysRevB.90.224104>
- [33] Q. Peng, Rahul, G. Wang, G.-R. Liu, S. Grimme, S. De, Predicting elastic properties of β -hmx from first-principles calculations, The Journal of Physical Chemistry B 119 (18) (2015) 5896–5903, pMID: 25906053. doi:10.1021/acs.jpcc.5b00083.
URL <http://dx.doi.org/10.1021/acs.jpcc.5b00083>
- [34] H. R., The elastic behaviour of a crystalline aggregate, Proceedings of the Physical Society. Section A 65 (5) (1952) 349.
URL <http://stacks.iop.org/0370-1298/65/i=5/a=307>
- [35] X.-Q. Chen, H. Niu, D. Li, Y. Li, Modeling hardness of polycrystalline materials and bulk metallic glasses, Intermetallics 19 (9) (2011) 1275 – 1281. doi:<http://doi.org/10.1016/j.intermet.2011.03.026>.
URL <http://www.sciencedirect.com/science/article/pii/S0966979511000987>

List of Figures

1	(Left) Monoclinic PEDOT crystal structure optimized at the PBEsol+D2 level. Carbon atoms are grey, oxygen red, sulfur yellow, hydrogen white. The crystallographic axes a , b , and c are marked in red, green and blue, respectively. (Center) View along the polymer chain. (Right) Brillouine zone and reciprocal point path for band structure.	12
2	Equation of state of PEDOT. (left) PBE+D2; (right) PBEsol+D2. The vertical dashed line indicates the equilibrium volume.	13
3	Band structure and density of states at equilibrium volume, obtained with PBE (top panel) and PBEsol (bottom panel). The horizontal red line indicates the top of the valence band. . .	14
4	Calculated elastic constants as a function of k-point sampling. The C_{22} and C_{33} have been rescaled for sake of clarity.	15
5	Calculated elastic properties as a function of k-point sampling.	16
6	Calculated directional elastic moduli. Solid lines correspond to maximum values. Dotted lines to minimum values. The polymeric chains are parallel to the y axis.	17

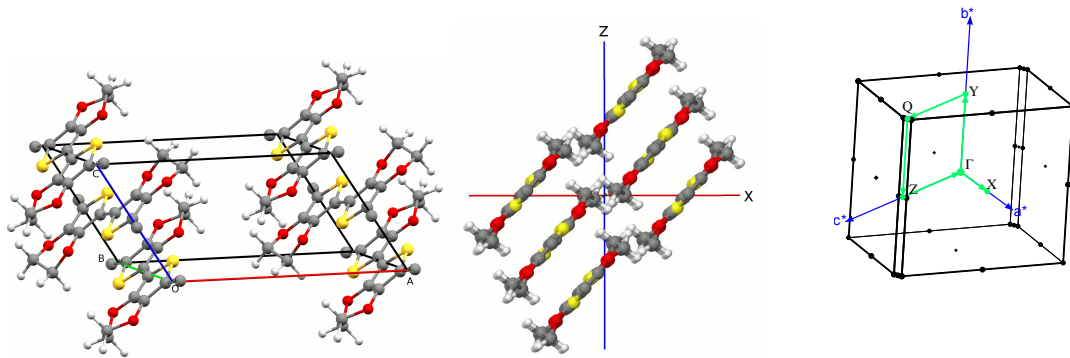


Figure 1: (Left) Monoclinic PEDOT crystal structure optimized at the PBEsol+D2 level. Carbon atoms are grey, oxygen red, sulfur yellow, hydrogen white. The crystallographic axes a , b , and c are marked in red, green and blue, respectively. (Center) View along the polymer chain. (Right) Brillouine zone and reciprocal point path for band structure.

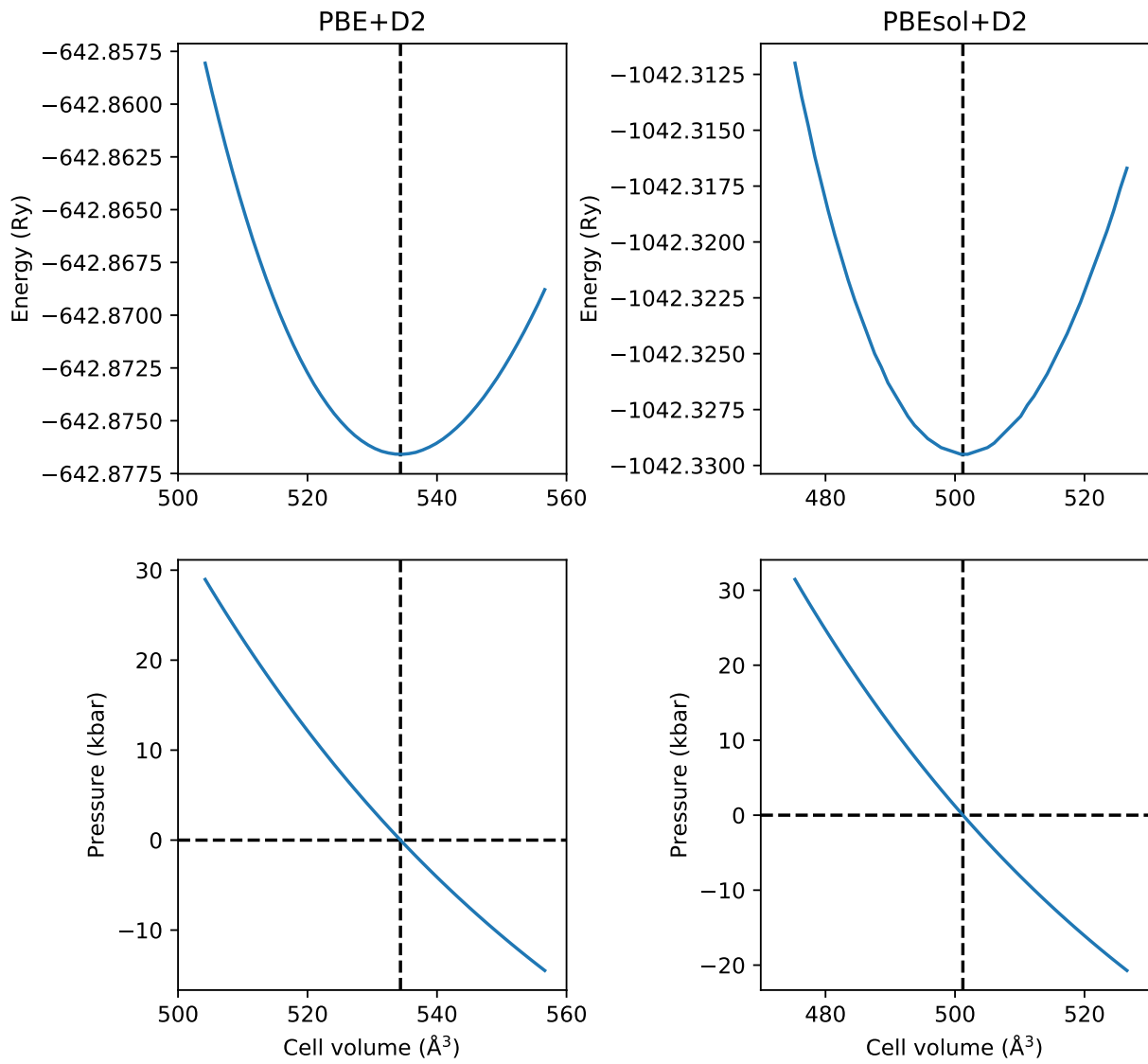


Figure 2: Equation of state of PEDOT. (left) PBE+D2; (right) PBEsol+D2. The vertical dashed line indicates the equilibrium volume.

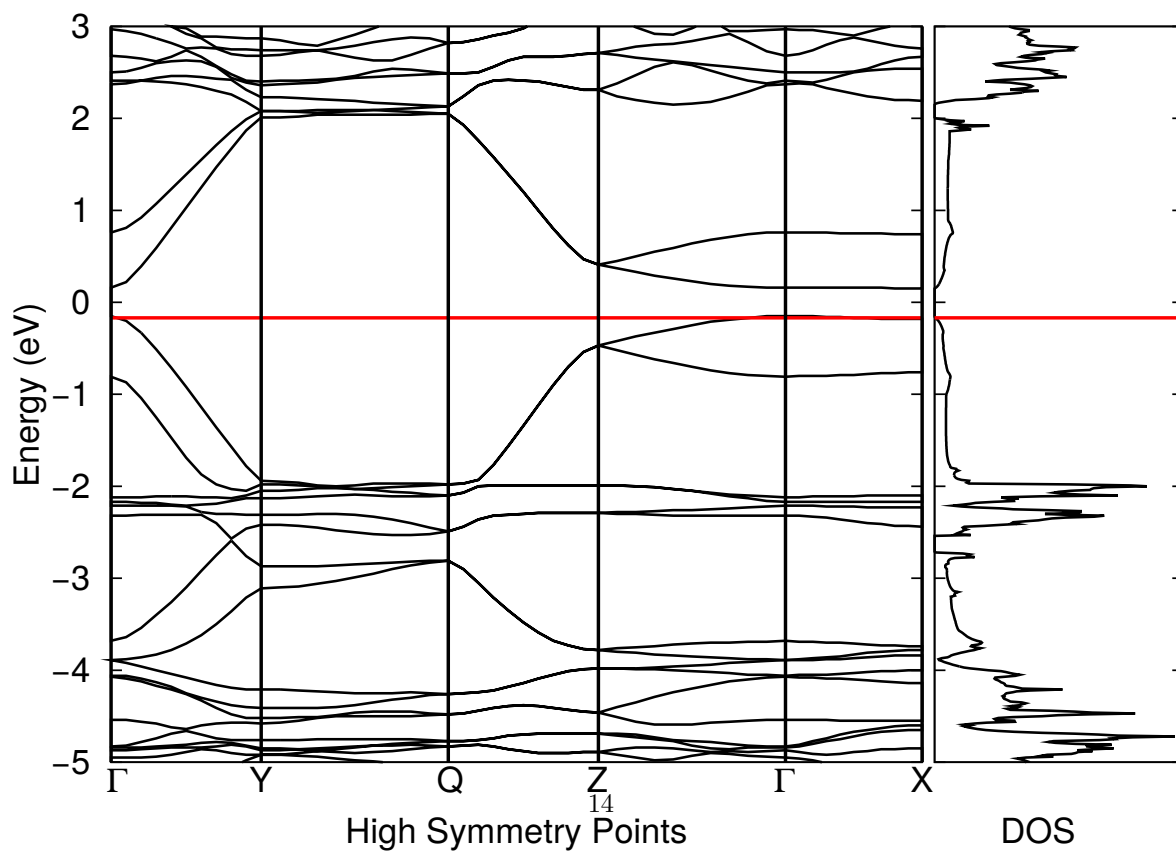
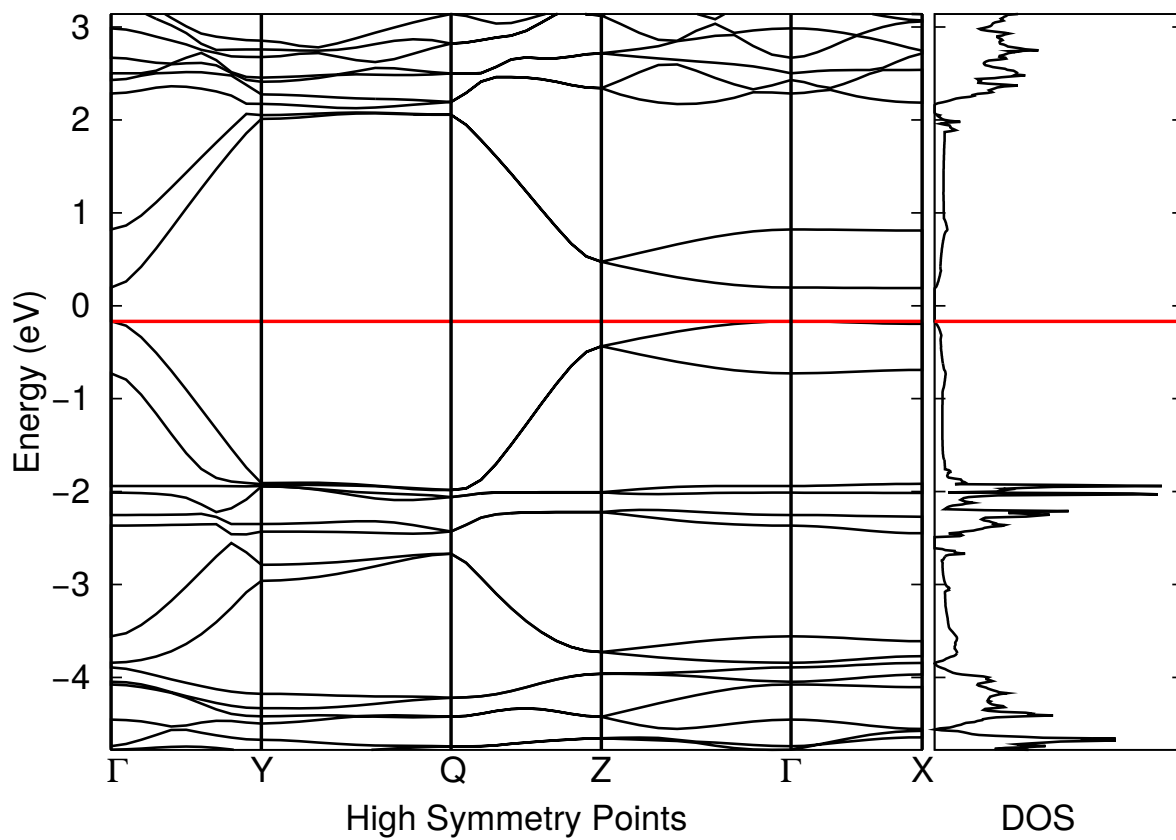


Figure 3: Band structure and density of states at equilibrium volume, obtained with PBE (top panel) and PBEsol (bottom panel). The horizontal red line indicates the top of the valence band.

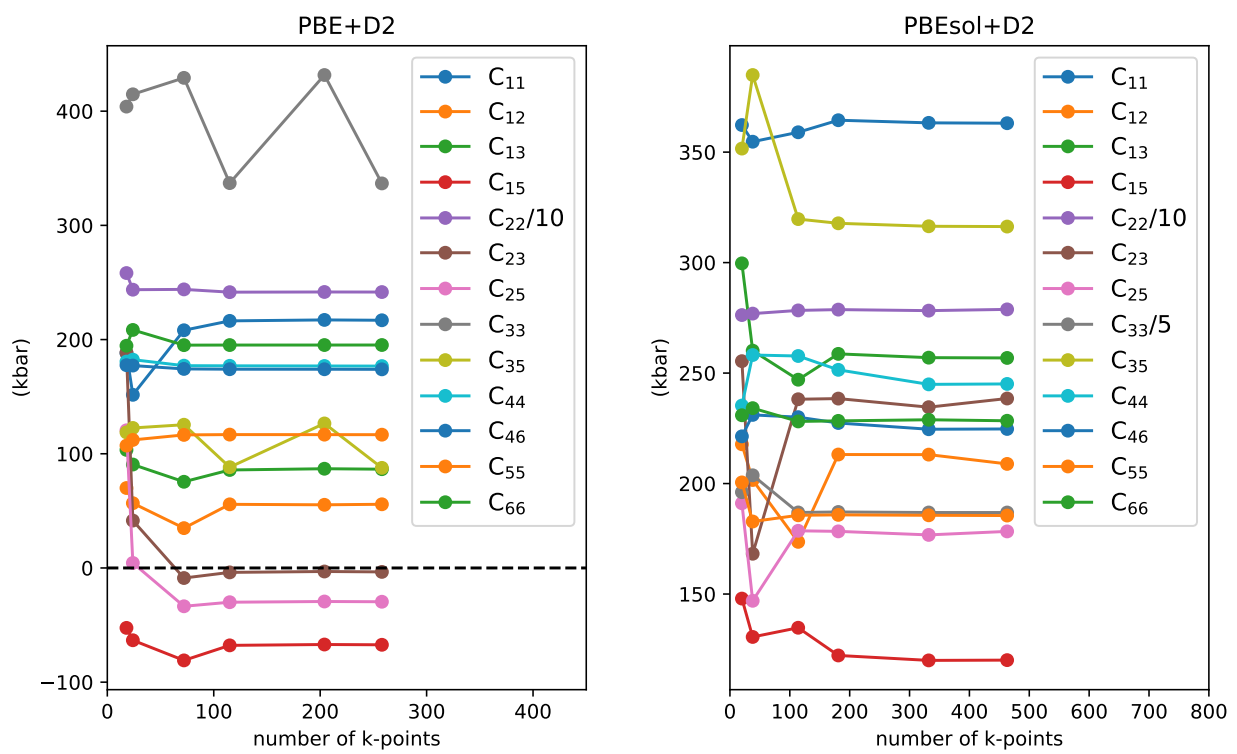


Figure 4: Calculated elastic constants as a function of k-point sampling. The C_{22} and C_{33} have been rescaled for sake of clarity.

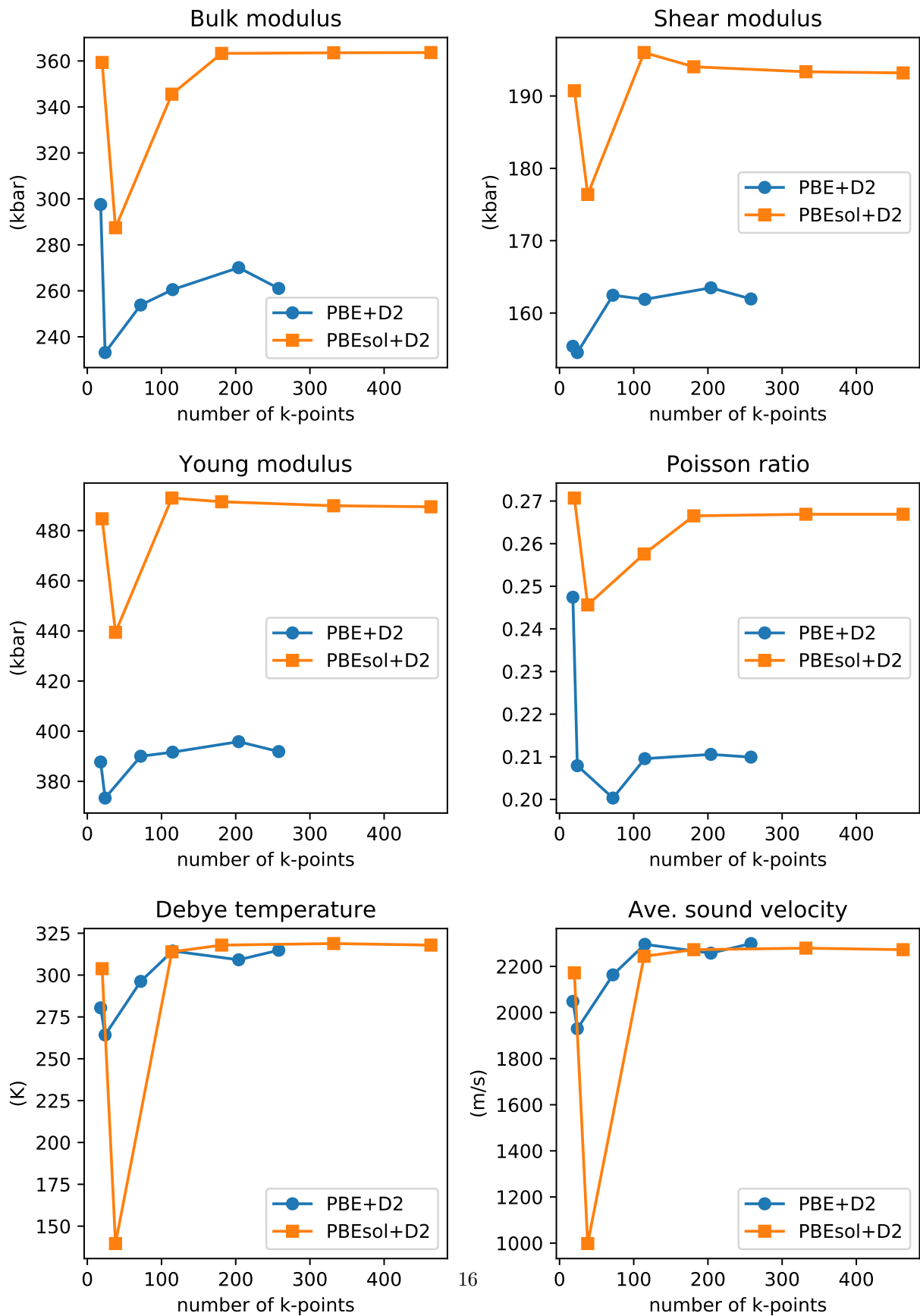


Figure 5: Calculated elastic properties as a function of k-point sampling.

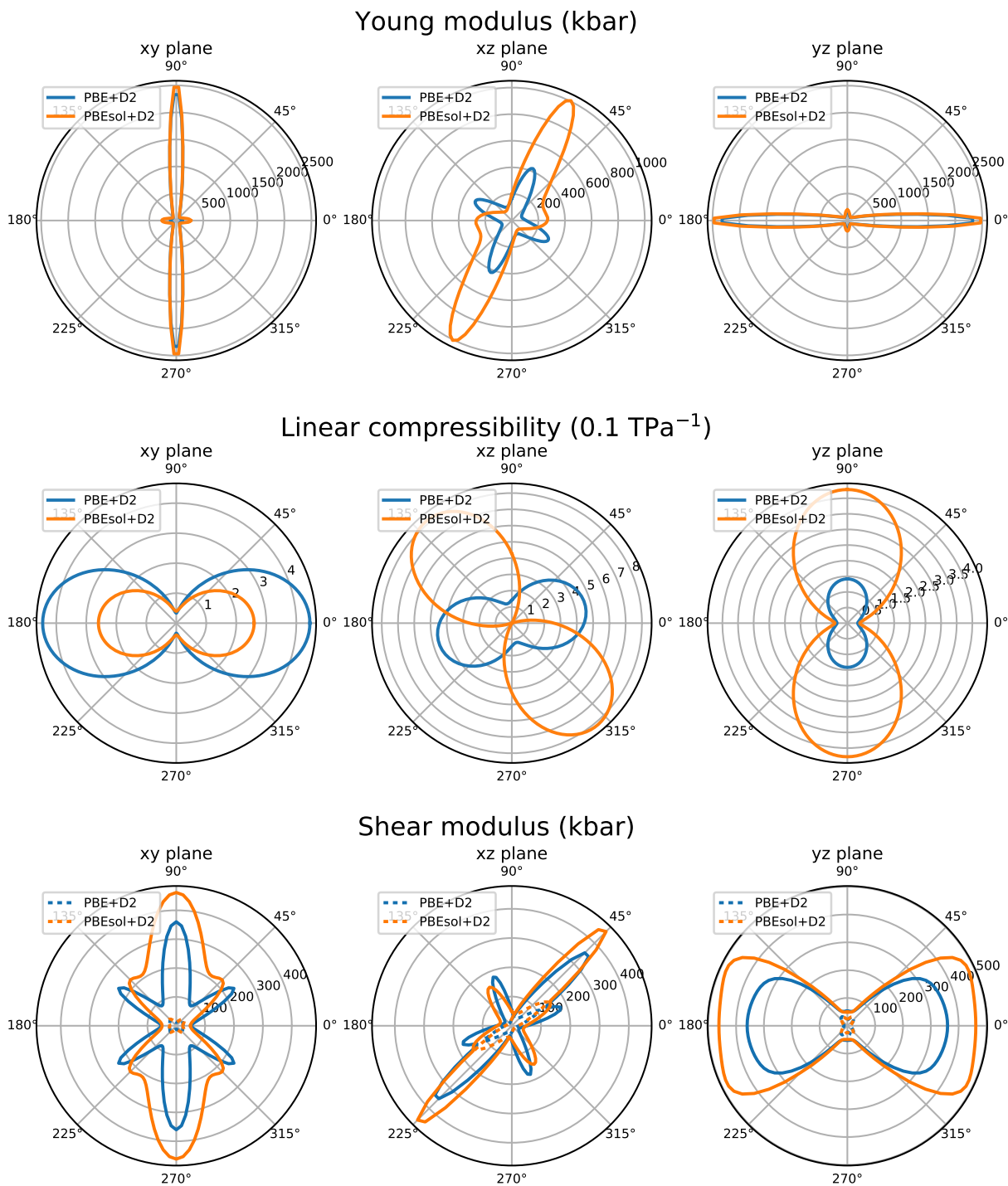


Figure 6: Calculated directional elastic moduli. Solid lines correspond to maximum values. Dotted lines to minimum values. The polymeric chains are parallel to the y axis.

List of Tables

1	Optimized lattice parameters of monoclinic PEDOT compared with experiments and other theoretical computation. a' , b' and c' are the lattice parameters of the orthorhombic structure. a , b , c and β are the lattice parameters of the monoclinic structure. PW=plane wave; NCPP=norm conserving pseudopotentials; USPP=ultrasoft pseudopotentials; PAW=projector augmented wave.	19
2	Comparison of band gap obtained in this work, previous calculations and experiments.	20
3	The 13 independent elastic constants, calculated using the PBE and PBEsol XC functionals	21
4	Computed Hill elastic moduli of crystalline PEDOT.	22

Method (XC functional)	a' (Å)	b' (Å)	c' (Å)	a (Å)	b (Å)	c (Å)	β (°)	Volume (Å ³)	Ref.
PW-NC (PBE)	–	–	–	10.843	7.878	7.465	124.1	556.08	This work
PW-PAW (PBEsol)	–	–	–	10.830	7.836	8.053	124.9	560.78	This work
PW-NC (PBE+D2)	–	–	–	10.773	7.878	7.445	123.0	534.36	This work
PW-PAW (PBEsol+D2)	–	–	–	10.173	7.826	7.438	122.3	501.22	This work
PW-USPP (PW91)	11.8	7.8	6.9	13.669	7.8	6.9	120.3	635.08	[10]
PW-NCPP (PBE)	10.52	7.935	7.6	12.978	7.935	7.6	125.8	634.42	[9, 11]
PW-PAW (PBE+D2)	–	–	–	12.000	7.820	7.040	123.0	554.05	[8]
Experiment	14.0	7.8	6.8	15.556	7.8	6.8	115.9	742.56	[7]
Experiment	10.52	7.87	5.66	12.052	7.87	5.88	119.2	468.60	[6]

Table 1: Optimized lattice parameters of monoclinic PEDOT compared with experiments and other theoretical computation. a' , b' and c' are the lattice parameters of the orthorhombic structure. a , b , c and β are the lattice parameters of the monoclinic structure. PW=plane wave; NCPP=norm conserving pseudopotentials; USPP=ultrasoft pseudopotentials; PAW=projector augmented wave.

Method	Type of PEDOT	Cryst. structure	Band gap (eV)	Ref.
PW-PP (PBE+D2)	undoped	monoclinic	0.42 (direct)	This work
PW-PAW (PBEsol+D2)	undoped	monoclinic	0.32 (direct)	This work
PW-PP (BLYP)	undoped	orthorhombic	0.37 (direct)	[11]
PW-USPP (PE)	undoped	orthorhombic	0.45 (direct)	[9]
PW-PAW (PBE+D2)	undoped	monoclinic	0.16 (direct)	[8]
PW-PAW (HSE06)	undoped	monoclinic	0.53 (direct)	[8]
Expt. (optical spectroscopy)	thin film		1.5–1.6	[5]
Expt. (vis-IR abs. spectra)	film		1.64	[12]
Expt. (spectroscopy, electrochemistry)	thin film	orthorhombic	~1.7	[6]

Table 2: Comparison of band gap obtained in this work, previous calculations and experiments.

Method	C_{11}	C_{12}	C_{13}	C_{15}	C_{22}	C_{23}	C_{25}	C_{33}	C_{35}	C_{44}	C_{46}	C_{55}	C_{66}
PBE+D2	216.9	55.8	86.5	-67.3	2416.1	-3.4	-29.6	336.7	87.7	176.8	173.9	116.7	95.2
PBEsol+D2	363.1	208.9	256.9	120.1	2788.2	238.5	178.3	747.6	361.3	245.0	224.7	185.5	228.4

Table 3: The 13 independent elastic constants, calculated using the PBE and PBEsol XC functionals

Method	Bulk modulus (kbar)	Shear modulus (kbar)	Young modulus (kbar)	Poisson ratio	Pugh ratio	Vicker's hardness (kbar)	Debye temperature (K)	Ave. speed of sound (m/s)
PBE+D2	261.0	161.0	391.9	0.2099	0.6203	19.4	315	2299.1
PBEsol+D2	363.7	193.2	489.5	0.2669	0.5312	17.7	318	2272.5

Table 4: Computed Hill elastic moduli of crystalline PEDOT.